Hindawi Publishing Corporation
Journal of Nanomaterials
Volume 2010, Article ID 203756, 7 pages
doi:10.1155/2010/203756

Research Article

Template-Based Electrochemically Controlled Growth of Segmented Multimetal Nanorods

Mee Rahn Kim, Dong Ki Lee, and Du-Jeon Jang

School of Chemistry, Seoul National University, NS60, Seoul 151-742, Republic of Korea

Correspondence should be addressed to Du-Jeon Jang, djjang@snu.ac.kr

Received 20 September 2010; Revised 19 November 2010; Accepted 10 December 2010

Academic Editor: Do Kim

Multisegmented one-dimensional nanostructures composed of gold, copper, and nickel have been fabricated by depositing metals electrochemically in the pores of anodic aluminum oxide (AAO) templates. The electrodeposition process has been carried out using a direct current in a two-electrode electrochemical cell, where a silver-evaporated AAO membrane and a platinum plate have served as a working electrode and a counter electrode, respectively. The striped multimetal rods with an average diameter of about 300 nm have tunable lengths ranging from a few hundred nanometers to a few micrometers. The lengths and the sequence of metal segments in a striped rod can be tailored readily by controlling the durations of electrodeposition and the order of electroplating solutions, respectively.

1. Introduction

Nanostructured materials have been extensively developed in fabrication methods and modified properties, and application ranges from fundamental science to industrial technology [1–9]. Metal nanoparticles are well known for their optical, electrical, thermal, catalytic, and magnetic properties as well as for biological interactions between some noble metals and biomolecules [10–15]. Especially, one-dimensional metallic nanostructures such as nanorods, nanowires, and nanotubes exhibit some advantages associated with their anisotropic architecture and allow to be employed as nanometer-scaled electronic devices and optoelectronic devices [15–17]. Due to their attractive potential in the miniaturization of devices and in the usage of bioanalysis, tremendous research efforts have been dedicated to their fabrication and modification [18–25]. Heterostructured metallic nanorods have been fabricated by many research groups because they can be used as electrocatalysts or nanobarcodes. For example, hybrid nanorods composed of electrocatalytically active metals such as platinum and nickel can have their maximum catalytic effects [24–26]. When the body of a metallic nanorod comprises longitudinally segmented metal sections, the heterostructured nanorod can be employed as a nanometer-scaled barcode [15, 24, 27].

The conventional methods of preparing one-dimensional metallic nanostructures are nanolithography and electrochemical deposition [28–32]. In particular, the electrochemical method has attracted much attention owing to its low cost, operation simplicity, and capability to deposit metallic materials into nanopores such as anodic aluminum oxide (AAO) membranes and polycarbonate membranes. AAO membranes have been easily and extensively employed not only as templates to fabricate one-dimensional nanostructures of wires and tubes, but also as masters to prepare ordered arrays of metal nanorings and regularly structured nanotextures [29–37]. AAO membranes are made by oxidizing aluminum sheets anodically in solutions of sulfuric, oxalic, and phosphoric acids, and they possess diverse advantages to be employed as templates [21, 32–34, 38]. First of all, they have uniform pores and parallel channels of large domains. Second, the diameters and lengths of their pores can be controlled easily and tailored finely. Third, AAO membranes offer a high thermal and mechanical stability, and they are chemically and thermally inert during the deposition of metals in the pores.

We have fabricated striped multimetal nanorods by electrodepositing three different metals of gold, copper, and nickel sequentially in the pores of AAO templates. A direct-current (DC) electrodeposition process has been carried

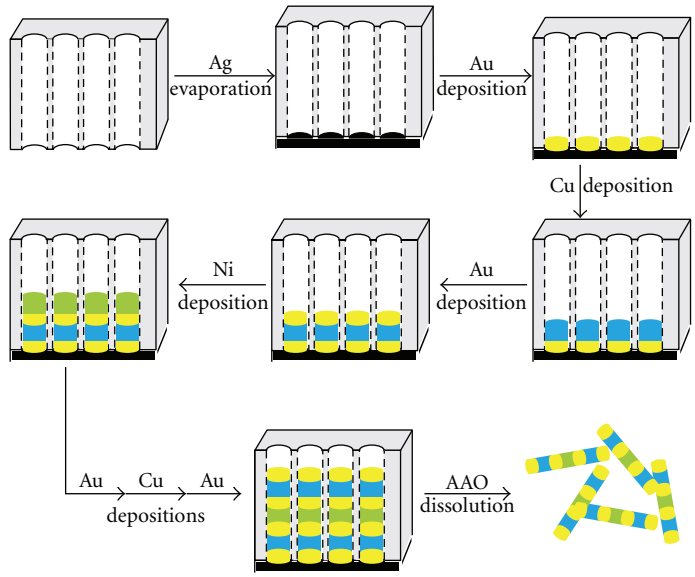

Figure 1: Schematically illustrated fabrication procedures of striped multimetal nanorods.

out in a two-electrode electrochemical cell system using a silver-baked AAO membrane as a working electrode and a platinum plate as a counter electrode. We will show that the lengths of metal segments in a striped rod, as well as the total length of the rod, can be tuned well by controlling the durations of electrodeposition.

2. Materials and Methods

2.1. Materials. The electroplating solutions of gold (technical gold 410), copper (technical copper PR), and nickel (high-speed nickel-sulfate process) were obtained from Hantech PMC. AAO membranes having the pore diameter of ~200 nm were purchased from Whatman International, and silver shots (99.999%) were from Sigma-Aldrich. For the preparation of a conductive AAO membrane, while an AAO membrane was placed on the holder of a thermal vacuum evaporator (Ultimate Vacuum, MHS-1800), silver shots were loaded on a tungsten boat and evaporated in a vacuum condition of 10^{-5} torr on the backside of the AAO membrane to have silver film thickness of 400 nm. The silver-evaporated AAO membrane was served as a working electrode of 0.5 cm^2 while a platinum plate was employed as a counter electrode of 1.5 cm^2. For the preparation of single-component metal nanorods, gold was electrodeposited at the anodic voltage of DC 4 V for 40 min under sonication at 45°C, nickel was at the anodic voltage of DC 3 V for 5 min under sonication at 45°C, and copper was at the anodic voltage of DC 2 V for 5 min at room temperature. For the fabrication of multimetal nanorods, gold and nickel metal segments were electrodeposited at the anodic voltage of DC 3 V under sonication at 45°C for 20 min and for 5 min, respectively, whereas copper was electrodeposited at the anodic voltage of DC 2 V at room temperature for 3 min. Each electrochemical deposition step requires the AAO membrane and the electrodeposition cell to be rinsed out completely. After finishing all the electrodeposition steps, we washed the specimen with water and dried it at 50°C. Free-standing metallic rods on a silver film were isolated by dissolving the AAO templates in 1 M NaOH for 1 h, while multimetal rods dispersed in a solution were prepared by removing the silver film of the specimen in a 12 M HCl solution for 30 s and by dissolving AAO templates subsequently in 1 M NaOH for 1 h.

2.2. Methods. Field-emission scanning electron microscopy (FESEM) images, energy-dispersive X-ray (EDX) spectra, and EDX elemental distribution maps were obtained with a microscope (JEOL, JSM-6700F) attached to a CCD camera as the detector. Reflectance spectra were measured using a UV/vis reflectance spectrometer (StellarNet, EPP2000C UV-VIS).

3. Results and Discussion

Figure 1 depicts a process flowchart for the fabrication of multimetal nanorods in a two-electrode cell system. After depositing silver thermally on the backsides of AAO membranes, we deposited three different metals electrochemically in the pores of the AAO membranes. At this stage, the electrochemical reduction of gold, copper, and nickel in electroplating solutions was carried out sequentially to prepare striped multimetal nanorods. The lengths of metal rods and the sequence of multimetal segments could be tuned easily by controlling the durations of electrodeposition and the order of electroplating solutions, respectively. Only the alumina membrane was removed after electrodeposition from the specimen to prepare free-standing rod structures, whereas both the alumina membrane and the silver film were removed from the specimen to prepare striped-metal rods dispersed in a solution. Single-component metal nanorods

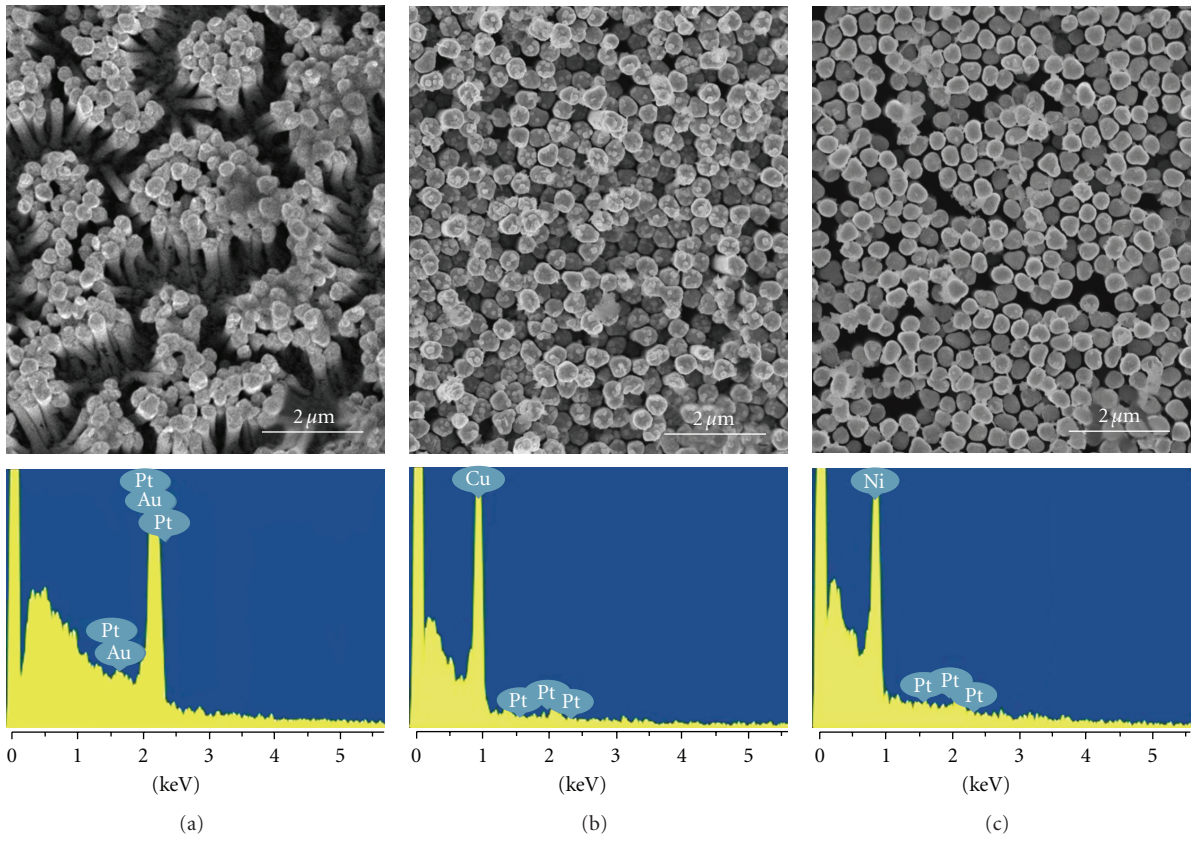

Figure 2: FESEM top-view images (top) and EDX spectra (bottom) of free-standing nanorods of gold (a), copper (b), and nickel (c) after removal of AAO templates by treatment with a 1.0 M NaOH solution for 1 h at room temperature.

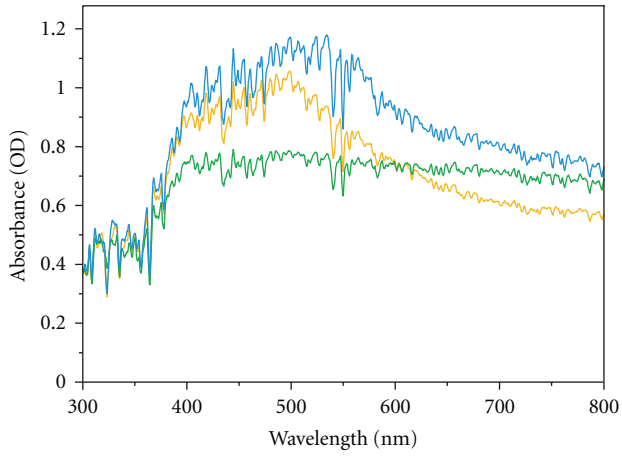

Figure 3: UV/vis reflectance spectra of the free-standing nanorods of gold (yellow), copper (blue), and nickel (green).

were fabricated by following the same above procedure in a metal electroplating solution.

Figure 2 shows that highly dense rod arrays of three different single-component metals are free-standing on Ag films. Each single-component metal nanorod array is well constructed, indicating that metal ions in an electroplating solution are introduced readily and reduced electrochemically in the nanopores of an AAO membrane. The elemental compositions of gold, copper, and nickel nanorods are evidenced by the EDX spectra of Figure 2 (where platinum also appears owing to contamination during Pt sputtering for FESEM measurements). The average diameters of produced gold, copper, and nickel rods are 300 ± 35, 383 ± 43, and 374 ± 40 nm, respectively, although the pore diameters of employed AAO membranes were ~200 nm. The average diameters of rods are different from one another depending on metals, and they are larger than the pore diameters of the employed templates. The templates of AAO membranes can be dissolved in strongly acidic or basic solutions [39, 40]. Because the electroplating solutions for the fabrication of metal rods are strongly acidic or basic, the walls of the AAO membranes were dissolved to some extent by electroplating solutions during electrodeposition. Thus, the diameters of metal nanorods produced in the templates were larger than the pore diameters of the original templates. We consider that the diameter of a nanorod increases with time because the AAO wall surrounding the rod dissolves slowly during electrodeposition. The pHs of the electroplating solutions of gold, copper, and nickel are 10, 3, and 4, respectively. In other words, the electroplating solutions of copper and nickel are acidic whereas the gold electroplating solution is basic. Thus, the copper and the nickel electroplating

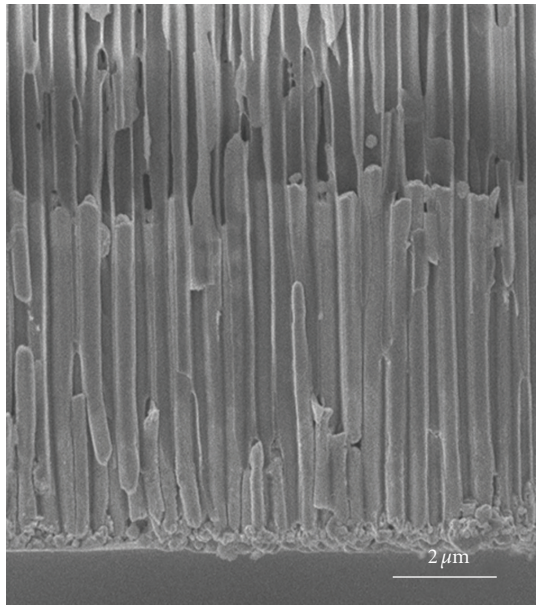

Element	Weight %	Atomic %
O K	21	47.3
Al K	22.7	30.2
Cu L	31.9	18
Pt M	10.7	2
Au M	13.7	2.5
Totals	100	100

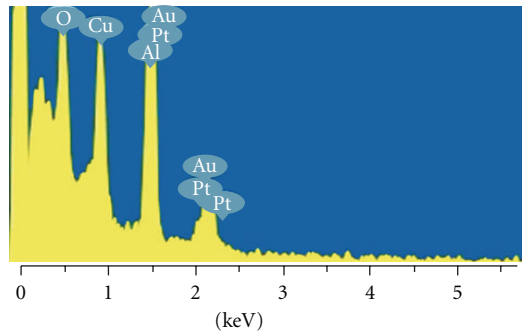

(a) (b)

Figure 4: FESEM image (a) and EDX data (b) of Au-Cu-Au nanorods embedded in an AAO membrane.

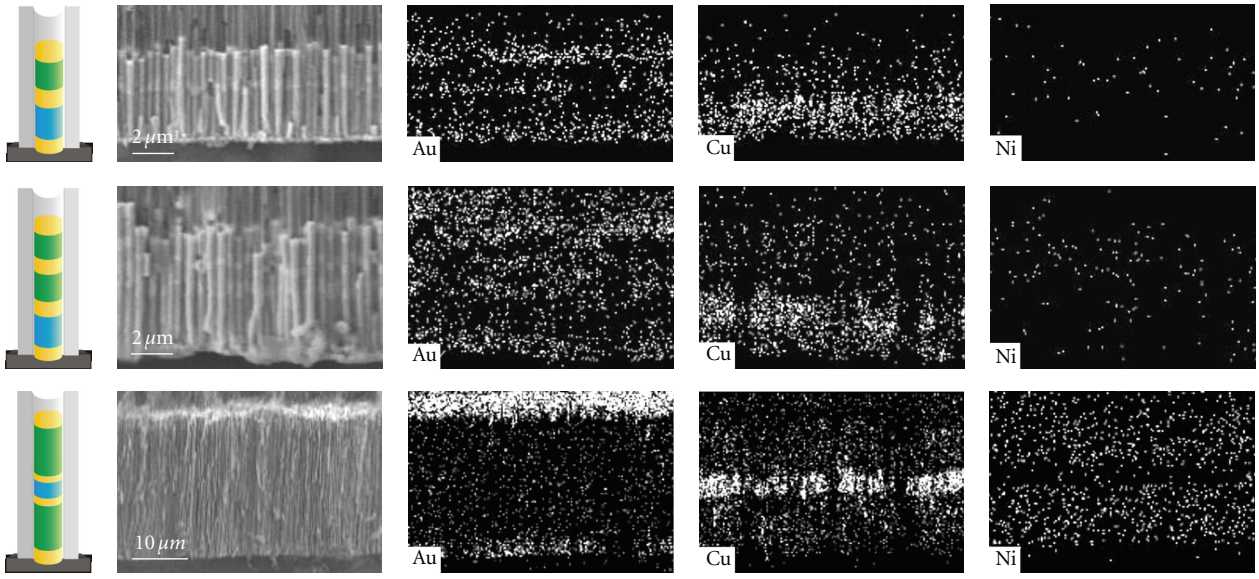

(a) (b) (c) (d) (e)

Figure 5: Illustrations (a), FESEM images (b), and EDX elemental distribution maps ((c), (d), and (e)) of Au-Cu-Au-Ni-Au (top), Au-Cu-Au-Ni-Au-Ni-Au (middle), and Au-Ni-Au-Cu-Au-Ni-Au nanorods (bottom) embedded in AAO membranes. Yellow, green, and blue colors in the illustrations denote gold, nickel, and copper, respectively.

solutions made the pore diameters of templates larger than the gold electroplating solution did, regardless of the dipping time during electrodeposition. The diameter of a segmented multimetal nanorod is considered to be not uniform: it may be the largest in the segment of copper and the smallest in the segment of gold.

The reflectance spectra of free-standing single-component metal nanorods in Figure 3 are very similar to the wavelength-dependent reflectance spectra of the respectively used bulk metals [14, 15] because the sizes of metal rods are too large to show quantum confinement effects in absorption. The absorption bands of gold and copper rods

have the maxima at 490 and 530 nm, respectively, whereas the absorption band of nickel rods has the maximum around 500 nm. Nevertheless, the reflectance spectra of free-standing metal nanorods in Figure 3 show the absorption characters of constituent metals well.

The FESEM image of Figure 4 indicates that multi-segment nanorods of Au-Cu-Au have been well constructed along the channels of an AAO membrane. The composite-metal nanorods have been fabricated based on the same technique used for the preparation of single-component rods of gold, copper, and nickel. Multimetal rods in the channels have similar lengths with no cracks generated from damages at interfaces between gold and copper segments. Although gold segments and copper segments are not distinguished in the FESEM image, the EDX data demonstrate that the multi-segment rods consist of gold and copper. Two metal components of the multimetal rods were not alloyed because the construction of gold and copper segments by electrochemical deposition was carried out sequentially in different baths. The elements of aluminum and oxygen originated from the templates because Au-Cu-Au nanorods were embedded in an AAO membrane whereas platinum resulted from Pt sputtering for the FESEM measurement.

Figure 5 designates that diverse segments of multi-metal nanorods have been fabricated by the sequential electrodeposition of gold, copper, and nickel metals. The FESEM images of hybrid metal rods embedded in AAO membranes show that the gold segments are contrastively brighter than the segments of copper or nickel. Multi-striped metal nanorods of Au-Cu-Au-Ni-Au and Au-Cu-Au-Ni-Au-Ni-Au have lengths of 6.6 and 9.1 μm, respectively. The EDX elemental distribution maps, corresponding to the FESEM images well, indicate that the individual segments of gold, copper, and nickel can be distinguishable in the multi-striped metal rods embedded in the AAO templates. Because the metal rods have the similar heights and exist in the templates, the segment arrays of each metal look like horizontal elemental bands. The EDX elemental distribution maps match well with the illustrations and FESEM images of striped-metal nanorods.

The EDX elemental distribution maps of Au-Cu-Au-Ni-Au nanorods (top row in Figure 5) show three horizontal gold bands and one horizontal copper band clearly. The elemental map of nickel, however, does not show any noticeable horizontal elemental band because, compared with the gold and copper, nickel has a low electron density. The interval between the first and the second horizontal gold bands from the bottom in the map can overlap to the horizontal copper band in the map, indicating that the striped multimetal rods are composed of metal segments. We can estimate the lengths of the respective metal segments of gold, copper, and nickel from obtained elemental distribution maps although the elemental distribution map of nickel is lacking in information. The estimated length of each gold segment is 1.0 μm whereas that of the copper segment, estimated by the gap between two horizontal gold bands from the bottom, is 2.0 μm. In addition, the length of the nickel segment having a featureless elemental intensity can be estimated as 1.5 μm via estimating the interval between two horizontal gold bands in the map. The metal height sum of 6.5 μm corresponds adequately to the measured total length of 6.6 μm for the Au-Cu-Au-Ni-Au rod. The elemental distribution maps of Au-Cu-Au-Ni-Au-Ni-Au nanorods (middle row in Figure 5) show four horizontal gold bands and one horizontal copper band. The horizontal copper band overlaps with the interval between two horizontal gold bands from the bottom in the map. We can estimate that the added total length of the rod is 9.0 μm, which accords with the measured value of 9.1 μm. The bottom row of Figure 5 shows that the long striped-metal rods of Au-Ni-Au-Cu-Au-Ni-Au have been also deposited electrochemically well at the same conditions, except for the quadruply elongated electrodeposition time of nickel. This implies that the lengths and orders of several metal segments can be controlled readily in order to fabricate striped-metal nanorods appropriate for applications. The length of the nickel segment was estimated to be 8 μm, and the segment-length sum of 22 μm was found to be similar to the measured length of 25 μm.

4. Conclusion

We have fabricated multi-segmented one-dimensional nanostructures composed of gold, copper, and nickel by depositing metals electrochemically in the pores of AAO templates. The electrodeposition process was carried out using DC in a two-electrode electrochemical cell, where a silver-evaporated AAO membrane and a platinum plate were employed as a working electrode and a counter electrode, respectively. The lengths of the striped multimetal rods with an average diameter of about 300 nm have been adjusted appropriately from a few hundred nanometers to a few micrometers by controlling the durations of electrodeposition. On the other hand, the sequence of metal segments in a striped nanorod was regulated by changing electroplating solutions during electrodeposition.

Acknowledgments

This work was supported by research grants through the National Research Foundation of Korea (NRF) funded by the Ministry of Education, Science, and Technology (2009-0082846 and 2010-0015806). D.-J. Jang is thankful to the SRC program of NRF (R11-2007-012-01002-0) and M. R. Kim acknowledges the BK21 scholarship.

References

[1] D. V. Talapin, J. S. Lee, M. V. Kovalenko, and E. V. Shevchenko, "Prospects of colloidal nanocrystals for electronic and optoelectronic applications," *Chemical Reviews*, vol. 110, no. 1, pp. 389–458, 2010.

[2] M. R. Kim, S. Y. Park, and D. J. Jang, "Facile controlled synthesis and spectroscopy of $CdS_{1-x}Se_x$ alloy and $(CdS)_{1-x}@(CdSe)_x$ core-shell nanotetrapods," *Advanced Functional Materials*, vol. 19, no. 24, pp. 3910–3916, 2009.

[3] R. D. Robinson, B. Sadtler, D. O. Demchenko, C. K. Erdonmez, L. W. Wang, and A. P. Alivisatos, "Spontaneous superlattice

formation in nanorods through partial cation exchange," *Science*, vol. 317, no. 5836, pp. 355–358, 2007.

[4] M. R. Kim, J. H. Chung, and D. J. Jang, "Spectroscopy and dynamics of Mn^{2+} in ZnS nanoparticles," *Physical Chemistry Chemical Physics*, vol. 11, no. 6, pp. 1003–1006, 2009.

[5] J. Goldberger, R. Fan, and P. Yang, "Inorganic nanotubes: a novel platform for nanofluidics," *Accounts of Chemical Research*, vol. 39, no. 4, pp. 239–248, 2006.

[6] M. R. Kim and D. J. Jang, "One-step fabrication of well-defined hollow CdS nanoboxes," *Chemical Communications*, no. 41, pp. 5218–5220, 2008.

[7] J. Y. Kim, S. Lee, K. H. Yoo, and D. J. Jang, "Coulomb blockade effect and negative differential resistance in the electronic transport of bacteriorhodopsin," *Applied Physics Letters*, vol. 94, no. 15, Article ID 153301, 2009.

[8] C. Harris and P. V. Kamat, "Photocatalysis with CdSe nanoparticles in confined media: mapping charge transfer events in the subpicosecond to second timescales," *ACS Nano*, vol. 3, no. 3, pp. 682–690, 2009.

[9] M. R. Kim, S. J. Kim, and D. J. Jang, "Fabrication of copper oxide nanoboxes containing a platinum nanocluster via an optical and galvanic route," *Crystal Growth and Design*, vol. 10, no. 1, pp. 257–261, 2010.

[10] Y. Tian, H. Liu, G. Zhao, and T. Tatsuma, "Shape-controlled electrodeposition of gold nanostructures," *Journal of Physical Chemistry B*, vol. 110, no. 46, pp. 23478–23481, 2006.

[11] J. Bisquert, "Physical electrochemistry of nanostructured devices," *Physical Chemistry Chemical Physics*, vol. 10, no. 1, pp. 49–72, 2008.

[12] R.-L. Zong, J. Zhou, B. Li, M. Fu, S.-K. Shi, and L.-T. Li, "Optical properties of transparent copper nanorod and nanowire arrays embedded in anodic alumina oxide," *Journal of Chemical Physics*, vol. 123, no. 9, Article ID 094710, 5 pages, 2005.

[13] H. Zhang, R. Jin, and C. A. Mirkin, "Synthesis of open-ended, cylindrical Au-Ag alloy nanostructures on a Si/SiO_x surface," *Nano Letters*, vol. 4, no. 8, pp. 1493–1495, 2004.

[14] S. R. Nicewarner-Peña, A. J. Carado, K. E. Shale, and C. D. Keating, "Barcoded metal nanowires: optical reflectivity and patterned fluorescence," *Journal of Physical Chemistry B*, vol. 107, no. 30, pp. 7360–7367, 2003.

[15] S. R. Nicewarner-Peña, R. G. Freeman, B. D. Reiss et al., "Submicrometer metallic barcodes," *Science*, vol. 294, no. 5540, pp. 137–141, 2001.

[16] Y. J. Liu, Z. Y. Zhang, Q. Zhao, R. A. Dluhy, and Y. P. Zhao, "Surface enhanced Raman scattering from an ag nanorod array substrate: the site dependent enhancement and layer absorbance effect," *Journal of Physical Chemistry C*, vol. 113, no. 22, pp. 9664–9669, 2009.

[17] S. Kim, K. L. Shuford, H. M. Bok, S. K. Kim, and S. Park, "Intraparticle surface plasmon coupling in quasi-one-dimensional nanostructures," *Nano Letters*, vol. 8, no. 3, pp. 800–804, 2008.

[18] X. Chen, H. Duan, Z. Zhou, J. Liang, and J. Gnanaraj, "Fabrication of free-standing Cu nanorod arrays on Cu disc by template-assisted electrodeposition," *Nanotechnology*, vol. 19, no. 36, Article ID 365306, 6 pages, 2008.

[19] M. Chen, L. Guo, R. Ravi, and P. C. Searson, "Kinetics of receptor directed assembly of multisegment nanowires," *Journal of Physical Chemistry B*, vol. 110, no. 1, pp. 211–217, 2006.

[20] J. B. Shi, Y. J. Chen, Y. T. Lin, C. Wu, C. J. Chen, and J. Y. Lin, "Synthesis and characteristics of Fe nanowires," *Japanese Journal of Applied Physics I*, vol. 45, no. 12, pp. 9075–9077, 2006.

[21] M. Lahav, E. A. Weiss, Q. Xu, and G. M. Whitesides, "Core-shell and segmented polymer-metal composite nanostructures," *Nano Letters*, vol. 6, no. 9, pp. 2166–2171, 2006.

[22] T. Mirkovic, M. L. Foo, A. C. Arsenault, S. Fournier-Bidoz, N. S. Zacharia, and G. A. Ozin, "Hinged nanorods made using a chemical approach to flexible nanostructures," *Nature Nanotechnology*, vol. 2, no. 9, pp. 565–569, 2007.

[23] E. D. Herderick, J. S. Tresback, A. L. Vasiliev, and N. P. Padture, "Template-directed synthesis, characterization and electrical properties of Au-TiO_2-Au heterojunction nanowires," *Nanotechnology*, vol. 18, no. 15, Article ID 155204, 6 pages, 2007.

[24] S. Park, S. W. Chung, and C. A. Mirkin, "Hybrid organic-inorganic, rod-shaped nanoresistors and diodes," *Journal of the American Chemical Society*, vol. 126, no. 38, pp. 11772–11773, 2004.

[25] S. H. Yoo and S. Park, "Platinum-coated, nanoporous gold nanorod arrays: synthesis and characterization," *Advanced Materials*, vol. 19, no. 12, pp. 1612–1615, 2007.

[26] H. M. Zhang, Y. G. Guo, L. J. Wan, and C. L. Bai, "Novel electrocatalytic activity in layered Ni-Cu nanowire arrays," *Chemical Communications*, vol. 9, no. 24, pp. 3022–3023, 2003.

[27] I. D. Walton, S. M. Norton, A. Balasingham et al., "Particles for multiplexed analysis in solution: detection and identification of striped metallic particles using optical microscopy," *Analytical Chemistry*, vol. 74, no. 10, pp. 2240–2247, 2002.

[28] A. Vlad, M. Mátéfi-Tempfli, V. A. Antohe et al., "Nanowire-decorated microscale metallic electrodes," *Small*, vol. 4, no. 5, pp. 557–560, 2008.

[29] Y. T. Pang, G. W. Meng, W. J. Shan et al., "Arrays of ordered Ag nanowires with different diameters in different areas embedded in one piece of anodic alumina membrane," *Applied Physics A*, vol. 77, no. 5, pp. 717–720, 2003.

[30] Z. F. Zhou, Y. C. Zhou, Y. Pan, and X. G. Wang, "Growth of the nickel nanorod arrays fabricated using electrochemical deposition on anodized Al templates," *Materials Letters*, vol. 62, no. 19, pp. 3419–3421, 2008.

[31] G. Cao and D. Liu, "Template-based synthesis of nanorod, nanowire, and nanotube arrays," *Advances in Colloid and Interface Science*, vol. 136, no. 1-2, pp. 45–64, 2008.

[32] N. Haberkorn, J. S. Gutmann, and P. Theato, "Template-assisted fabrication of free-standing nanorod arrays of a hole-conducting cross-linked triphenylamine derivative: toward ordered bulk-heterojunction solar cells," *ACS Nano*, vol. 3, no. 6, pp. 1415–1422, 2009.

[33] J. H. Lee, J. H. Wu, H. L. Liu et al., "Iron-gold barcode nanowires," *Angewandte Chemie—International Edition*, vol. 46, no. 20, pp. 3663–3667, 2007.

[34] H. D. Yan, P. Lemmens, H. Dierke, S. C. White, F. Ludwig, and M. Schilling, "Iron/nickel nanowires growth in anodic aluminum oxide templates: transfer of length scales and periodicity," *Journal of Physics: Conference Series*, vol. 145, Article ID 012079, 2009.

[35] C. W. Huang and Y. W. Hao, "The fabrication of short metallic nanotubes by templated electrodeposition," *Nanotechnology*, vol. 20, no. 44, Article ID 445607, 7 pages, 2009.

[36] S. H. Yoo, L. Liu, and S. Park, "Nanoparticle films as a conducting layer for anodic aluminum oxide template-assisted nanorod synthesis," *Journal of Colloid and Interface Science*, vol. 339, no. 1, pp. 183–186, 2009.

[37] M. R. Kim, S. Y. Heo, and D. J. Jang, "Nanopattern transfer and wettability modification of regularly structured metallic

and polymeric surfaces with replication," *Journal of Colloid and Interface Science*, vol. 339, no. 1, pp. 217–221, 2009.

[38] M. R. Kim, J. Y. Kim, and D. J. Jang, "Electrochemical fabrication of arrayed alumina nanowires showing strong blue emission," *European Physical Journal D*, vol. 43, no. 1–3, pp. 279–282, 2007.

[39] Y. T. Tian, G. W. Meng, T. Gao et al., "Alumina nanowire arrays standing on a porous anodic alumina membrane," *Nanotechnology*, vol. 15, no. 1, pp. 189–191, 2004.

[40] Z. L. Xiao, C. Y. Han, U. Welp et al., "Fabrication of alumina nanotubes and nanowires by etching porous alumina membranes," *Nano Letters*, vol. 2, no. 11, pp. 1293–1297, 2002.